Journal of Microbiology (2014) Vol. 52, No. 11, pp. 970–975
DOI 10.1007/s12275-014-4323-6

Function of VP2 Protein in the Stability of the Secondary Structure of Virus-like Particles of Genogroup II Norovirus at Different pH Levels: Function of VP2 Protein in the Stability of NoV VLPs

Yao Lin, Li Fengling, Wang Lianzhu, Zhai Yuxiu, and Jiang Yanhua*

Key Laboratory of Test and Evaluation on Quality and Safety of Aquatic Products, Ministry of Agriculture, Yellow Sea Fisheries Research Institute, Chinese Academy of Fishery Sciences, Qingdao 266071, P. R. China

(Received Jun 5, 2014 / Revised Aug 27, 2014 / Accepted Aug 28, 2014)

VP2 is the minor structural protein of noroviruses (NoV) and may function in NoV particle stability. To determine the function of VP2 in the stability of the NoV particle, we constructed and purified two kinds of virus-like particles (VLPs), namely, VLPs (VP1) and VLPs (VP1+VP2), from Sf9 cells infected with recombinant baculoviruses by using a Bac-to-Bac® baculovirus expression system. The two kinds of VLPs were treated with different phosphate buffers (pH 2 to pH 8); the secondary structure was then analyzed by far UV circular dichroism (CD) spectroscopy. Results showed that significant disruptions of the secondary structure of proteins were not observed at pH 2 to pH 7. At pH 8, the percentages of α-helix, β-sheet, and β-turn in VLPs (VP1) were decreased from 11% to 8%, from 37% to 32%, and from 20% to 16%, respectively. The percentage of coil was increased from 32% to 44%. By contrast, the percentages of α-helix, β-sheet, and β-turn in VLPs (VP1+VP2) were decreased from 11% to 10%, from 37% to 35%, and from 20% to 19%, respectively. The percentage of coil was increased from 32% to 36%. VLPs (VP1+VP2) was likely more stable than VLPs (VP1), as indicated by the percentage of the secondary structures analyzed by CD. These results suggested that VP2 could stabilize the secondary structure of VLPs under alkaline pH conditions. This study provided novel insights into the molecular mechanism of the function of VP2 in the stability of NoV particles.

Keywords: norovirus, virus-like particle, stability, VP2, secondary structure, circular dichroism spectroscopy

Introduction

Norovirus (NoV) is a genus belonging to the family *Caliciviridae* and recognized as one of the most common agents of infectious gastroenteritis among persons of all ages (Widdowson *et al*., 2005). The NoV genus is further subdivided into five genogroups (GI to GV) based on sequence information of genes encoding viral RNA-dependent RNA polymerase and capsid protein (Zheng *et al*., 2006). Three of these genogroups, particularly I, II, and IV, are found in humans (Ando *et al*., 2000; Karst *et al*., 2003); among these genogroups, genogroup II viruses (more precisely, genogroup II.4 NoV) is the most prevalent (Atmar and Estes, 2006; Svraka *et al*., 2007; Kroneman *et al*., 2008). The NoV genome consists of a single-stranded positive-sense RNA of approximately 7.6 kb organized into three open reading frames (ORF): ORF1 encodes non-structural proteins; ORF2 encodes the major capsid protein VP1; and ORF3 encodes the minor structural protein VP2 (Jiang *et al*., 1993).

NoV cannot be cultivated in cell culture, and no animal model has been established yet. As such, studies of NoV have been impeded. When expressed in insect cells using a baculovirus expression system, the capsid protein VP1 spontaneously forms empty virus-like particles (VLPs) without RNA, and these particles structurally and antigenically mimic the native virus except they do not contain RNA (Jiang *et al*., 1992). VLPs can be expressed and purified in relatively high yields. Furthermore, these particles are the source of data regarding the structural and functional domains of VP1 and NoV capsids.

NoV is stable in the environment and retains its infectivity even after this virus is exposed to pH 2.7 for 3 h and after it is heated at 60°C for 30 min (Pirtle and Beran, 1991). The NoV surrogate feline calicivirus shows that VLPs are stable at room temperature for more than 20 d and at 4°C for 60 d when these particles are dried on a surface. Infectious virus titers have been detected even after feline calicivirus is heated at 70°C for 3 min (Doultree *et al*., 1999). Although VLPs assemble in the absence of VP2, evidence suggests that VP2 may function in particle stability (Bertolotti-Ciarlet *et al*., 2002). However, the exact function of VP2 in NoV particles remains unknown.

In the present study, the function of the VP2 protein in the stability of the secondary structure of NoV VLPs was investigated by circular dichroism spectroscopy (CD). The results of the study provided new insights into the function of NoV VP2.

Materials and Methods

Construction of recombinant baculovirus for VP1 and VP2

pMD-ORF2 and pMD-ORF3 plasmids, which contained the

*For correspondence. E-mail: jiangyanhua2011@126.com; Tel./Fax: +86-0532-85821813

VP1 gene (GenBank EF535854) and the VP2 gene (GenBank EF635440) of genogroup II NoV, respectively, were kindly provided by Dr. Wang (Shang Hai Jiao Tong University, China). The primers used to generate the ORF2 of NoV were pNVORF2f (5′-TTTGTCGACATGAAGATGGCGACGAATGACG-3′) and pNVORF2r (5′-TTTGGTACCTAATGCACGTCTACGC-3′) containing restriction enzyme sites (underlined). The PCR mixture of ORF2 contained 1.0 μl of plasmid pMD-ORF2, 2.0 U *Taq* DNA polymerase (Fermentas, Canada), 5.0 μl of 10× *Taq* buffer (with Mg^{2+}), 1.0 μl of 10.0 mM dNTPs, and 1.0 μl of 10.0 mM primers (pNVORF2f and pNVORF2r). Deionized water was also added to obtain the final volume of 50.0 μl. The ORF2 amplification conditions were listed as follows: initial denaturation at 94°C for 5 min; denaturation for 30 sec at 94°C; annealing for 50 sec at 55°C; and extension for 2 min at 72°C for 30 cycles with additional 7 min of extension at 72°C.

The primers used to generate the ORF3 of NoV were pNVORF3f (5′-TTTGTCGACATGGCTGGGGCTTTCTTTGC-3′) and pNVORF3r (5′-TTTGGTACCTAA*GTGATGGTGATGGTGATG*CGCCCGTGACTCC-3′) containing restriction enzyme sites and 6×His tag (italicized). The PCR mixture of ORF3 contained 1.0 μl of plasmid pMD-ORF3, 2.0 U *Taq* DNA polymerase (Fermentas, Canada), 5.0 μl 10× *Taq* buffer (with Mg^{2+}), 1.0 μl of 10.0 mM dNTPs, and 1.0 μl of 10.0 mM primers (pNVORF3f and pNVORF3r). Deionized water was also added to obtain the final volume of 50.0 μl. The ORF3 amplification conditions were listed as follows: initial denaturation at 94°C for 5 min; denaturation for 30 sec at 94°C; annealing for 40 sec at 56°C; and extension for 1 min at 72°C for 30 cycles with additional 7 min of extension at 72°C.

The PCR-generated ORF2 or ORF3 fragment digested with *Sal*I and *Kpn*I was ligated in a previously *Sal*I- and *Kpn*I-digested baculovirus transfer vector pFastBac to generate the recombined transfer vectors. The recombinant baculovirus expressions of VP1 and VP2 were generated in Sf9 cells (*Spodoptera frugiperda* ovarian cell line) by using a Bac-to-Bac® baculovirus expression system (Invitrogen, USA) in accordance with the manufacturer's instructions. Recombinant baculoviruses were plaque-purified twice before infection was induced in Sf9 cells. Two clones of each recombinant baculovirus (Bac-VP1 and Bac-VP2) were subjected to PCR and confirmed that these clones contained the target DNA; the following M13 primers were used according to the recommended protocol: M13F 5′-GTTTTCCCAGTCACGAC-3′ and M13R 5′-CAGGAAACAGCTATGAC-3′.

Expression and purification of VLPs

The recombinant baculovirus stock Bac-VP1 was generated and monolayers of Sf9 insect cells were infected at a multiplicity of infection (MOI) of 5 to obtain VLPs (VP1) without VP2. At 5 d post-infection, cells and supernatants were harvested and subjected to three freezing/thawing cycles. Cell lysates were centrifuged at 5,000 × *g* for 15 min to separate the cell debris. Clear supernatants were centrifuged again at 10,000 × *g* for 30 min to spin down large protein complexes or baculovirus particles. The VLPs in the supernatant were then purified by centrifugation at 100,000 × *g* for 150 min. To purify VLPs, we separated the resuspended pellets by sucrose step gradient (5% to 45%) centrifugation (Jiang *et al*., 1992, 1995). The pellet was resuspended in sterile water and then stored at 4°C until further use. Purity was assessed by SDS-PAGE and Coomassie staining.

Sf9 cells were dually infected with Bac-VP1 and Bac-VP2 to obtain VLPs (VP1+VP2) containing VP2. Each recombinant baculovirus was administered at MOI of 5 according to a previously described method (Glass *et al*., 2000). VLPs (VP1+VP2) were purified using the same protocol described above.

Western blot analysis

Ultracentrifugation-purified VLPs (VP1) or VLPs (VP1+VP2) were separated by sodium dodecyl sulfate-polyacrylamide gel electrophoresis (SDS-PAGE). In western blot analysis, proteins were transferred to a nitrocellulose membrane according to a previously described method (Wang *et al*., 2008). In brief, the membrane was blocked with 1% bovine serum albumin (Sigma) overnight at room temperature with agitation. Afterward, this membrane was washed thrice with phosphate-buffered saline (PBS) containing 0.1% (v/v) Tween 20 (PBS-T) and then incubated with the first antibody 12F4 (1:1000) (Wang *et al*., 2008) against VP1 or anti-6×His tag monoclonal antibody (1:1000; Tiangen Biotech Co., Ltd., China) at 37°C for 30 min. After rinsing with PBS-T, the membrane was incubated with horseradish peroxidase (HRP) conjugated goat anti-mouse IgG (1:10000; Tiangen Biotech Co., Ltd.). Western blot reactivity was developed using an enhanced HRP-DAB chromogenic substrate kit (Tiangen Biotech Co., Ltd.). Sf9 cells infected with wild-type baculovirus and uninfected Sf9 cells were used as control samples in western blot analysis.

Electron Microscopy (EM)

The prepared VLPs were stained with 2% uranyl acetate and then examined under an electron microscope (H-7650, HITACHI) at a magnification of 50,000×.

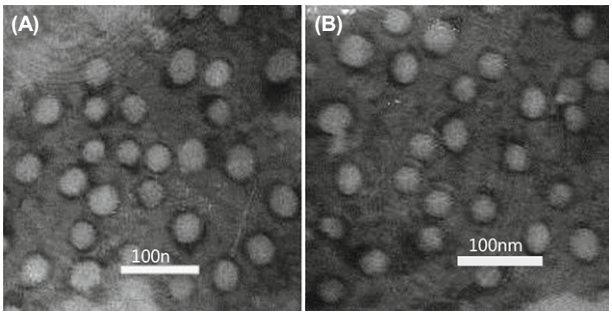

Fig. 1. Electron micrographs of VLPs (VP1) and VLPs (VP1+VP2). (A) VLPs (VP1), virus-like particles composed of VP1 alone, from Sf9 cells infected by recombinant baculoviruses Bac-VP1, ultracentrifugation-purified by sucrose step gradient, negative stained; (B) VLPs (VP1+VP2), composed of VP1 and VP2, which are obtained from Sf9 cells dually infected by recombinant baculoviruses Bac-VP1 and Bac-VP2, ultracentrifugation-purified by sucrose step gradient, negative stained. The size of the two kinds of VLPs is approximate 38 nm, and no evident morphological difference between the two kinds of VLPs.

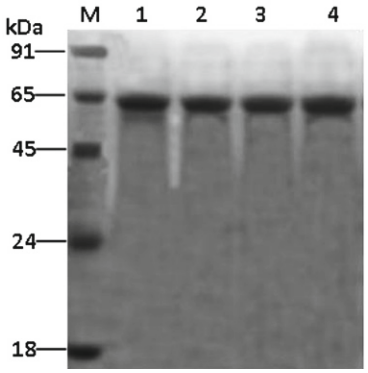

Fig. 2. Sodium dodecyl sulfate-polyacrylamide gel electrophoresis (SDS-PAGE) analysis of VLPs (VP1) and VLPs (VP1+VP2). Purified VLPs (VP1) and VLPs (VP1+VP2) were analyzed by SDS-AGE. Lanes: M, protein marker; 1 and 2, Purified VLPs (VP1); 3 and 4, Purified VLPs (VP1+VP2). Both VLPs (VP1) and VLPs (VP1+VP2) show 58 kDa bands, however, VLPs (VP1+ P2) did not show 23 kDa band, as expected.

Secondary structure analysis

Purified VLPs (VP1) and VLPs (VP1+VP2) were treated with phosphate buffer at different pH levels (pH 2 to pH 8) for 1 h at room temperature. Afterward, these VLPs were analyzed by far UV CD spectroscopy using Jasco 810 spectropolarimeter (Jasco Inc., Japan) equipped with a computer (Ausar *et al.*, 2006). VLPs solutions were prepared at a protein concentration of 0.22 mg/ml and placed in 0.1 cm path length stoppered quartz cuvettes. Spectra were obtained at a resolution of 0.5 nm and a scanning speed of 20 nm/min with a response time of 2 sec and a bandwidth of 1 nm. Each spectrum corresponded to an average of six independent scans. The secondary structures of the two kinds of VLPs were analyzed with Spectra Manager™ II software (Jasco Inc.) based on a previously described model (Yang *et al.*, 1986).

Results

Construction of recombinant baculovirus to produce VP1 and VP2

The recombinant baculoviruses Bac-VP1 and Bac-VP2 were constructed according to the manufacturer's manual of the Bac-to-Bac® baculovirus expression system. The VLPs (VP1) was purified from Sf9 cells infected by Bac-VP1 and examined by EM (Fig. 1 A), SDS-PAGE (Fig. 2, Line 1 and 2), and western blot (Fig. 3). VP1 with typical NoV morphological characteristics was observed in negatively stained EM grids prepared from the peak fractions containing 58 kDa capsid proteins.

The VLPs (VP1+VP2) was purified from Sf9 cells dually infected with Bac-VP1 and Bac-VP2. EM (Fig. 1B) and SDS-PAGE (Fig. 2, Lines 3 and 4) results showed that the VLPs (VP1) and the VLPs (VP1+VP2) did not differ. However, western blot results showed that VLPs (VP1+VP2) exhibited a 23 kDa band, indicating the presence of VP2 in the VLPs (VP1+VP2) (Fig. 4).

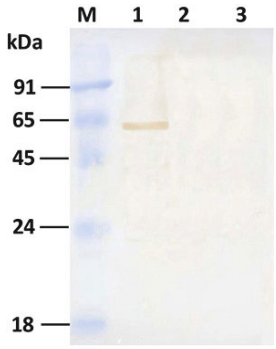

Fig. 3. Western blot analysis of VLPs (VP1). VLPs (VP1) were transferred to a nitrocellulose membrane after separated by sodium dodecyl sulfate-polyacrylamide gel electrophoresis (SDS-PAGE), incubated with the first antibody against VP1, followed by the second antibody conjugated horseradish peroxidase. Lanes: M, Prestained protein marker; 1, Purified VLPs (VP1), which showed a specific protein band at nearly 58 kDa; 2 and 3, Negative control, Sf9 cells infected with wild-type baculovirus and uninfected Sf9 cells respectively, which showed no bands at all.

Secondary structure analysis of 2 kinds of VLPs

The stability of the secondary structure of the two kinds of VLPs in buffers with different pH levels was analyzed by CD. The spectrum of VLPs composed of VP1 at pH 7 showed a single negative spike at approximately 205 nm and two weak positive maxima at approximately 193 nm and 233 nm. These spectral characteristics suggested that the VP1 protein contained a significant amount of β-sheet. Secondary structure analysis (Yang *et al.*, 1986) revealed that the percentages of α-helix and β-sheet were 11% and 37%, respectively. These results are in good agreement with crystallographic data (Prasad *et al.*, 1999) and CD spectrum data available for VP1 (Ausar *et al.*, 2006). The percentages of β-turn and coil were 20% and 32%, respectively. Similar spectra were obtained, indicating that these secondary structures were not significantly disrupted at pH 2 to pH 6. At pH 8, the percentages of α-helix, β-sheet, and β-turn in VP1 were decreased from 11% to 8%, from 37% to 32%, and from 20% to 16%, respectively. By contrast, the percentage of coil was increased from 32% to 44%. The minima in the observed CD spectrum at pH 8 shifted from 205 nm to 200 nm, which differed from that in the CD spectrum obtained at pH 2 to pH 7, in which a minima shift accureed from 205 nm to 202 nm (Fig. 5).

The spectrum of VLPs (VP1+VP2) at pH 7 did not evidently differ from that of VLPs (VP1) (data not shown), and the percentage of each secondary structure was the same as that of VP1. The same result was also observed at other pH levels except pH 8. At pH 8, the percentages of α-helix, β-sheet, and β-turn were decreased from 11% to 10%, from 37% to 35%, and from 20% to 19%, respectively. The per-

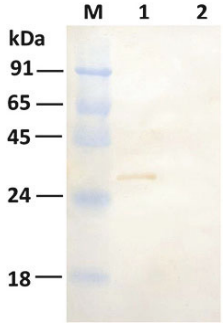

Fig. 4. Western blot analysis of the VP2 in VLPs (VP1+VP2). Purified VLPs (VP1+VP2) were analysised by western blot to detect the VP2 protein. VLPs (VP1+VP2) were transferred to a nitrocellulose membrane after separated by SDS-PAGE, incubated with the anti-6×His tag monoclonal antibody, followed by the second antibody conjugated horseradish peroxidase. Lanes: M, Prestained protein marker; 1, Purified VLPs (VP1+VP2), which showed a specific protein band at nearly 23 kDa; 2, Negative control, uninfected Sf9 cells, which showed no bands at all.

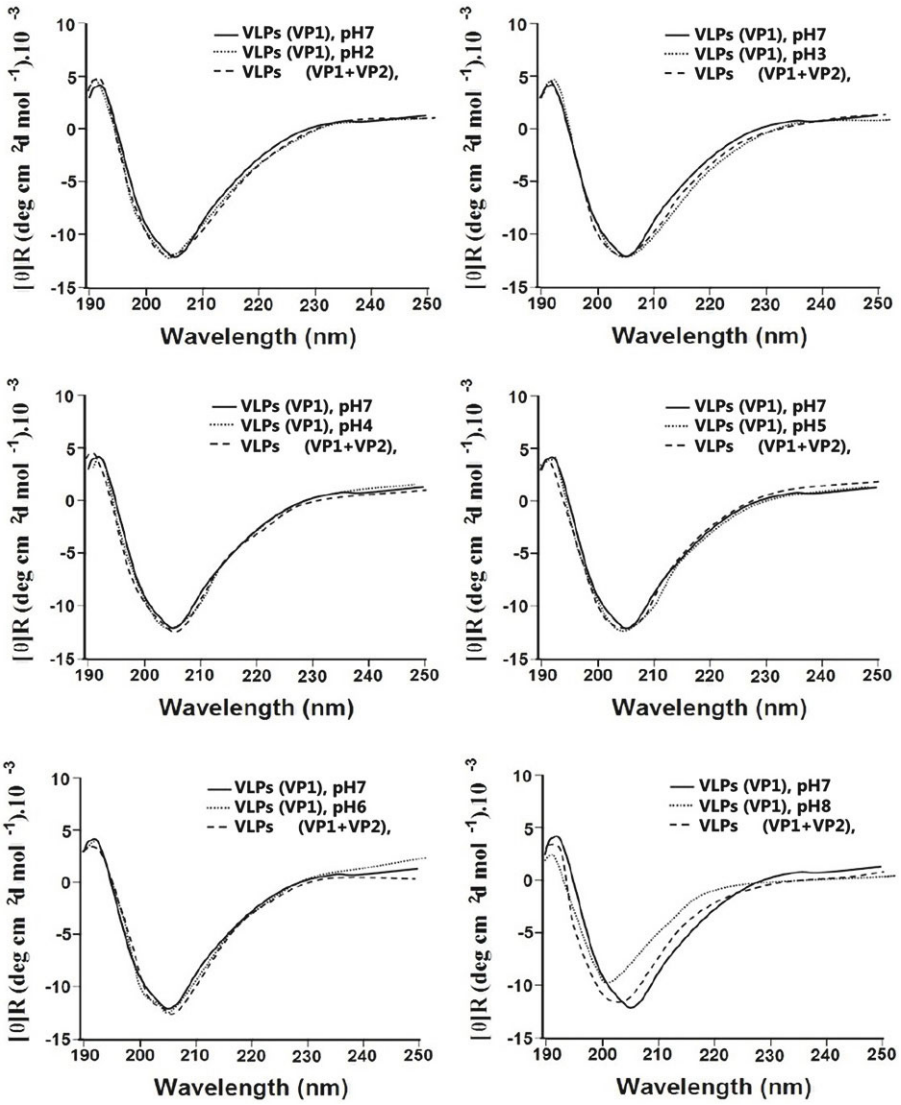

Fig. 5. Circular dichroism (CD) spectra of VLPs (VP1) and VLPs (VP1+VP2) at pH 2 to pH 8. X-axis: the scanning wavelength; Y-axis: the CD value. At pH 2 to pH 7, no evident difference in CD spectra between VLPs (VP1) and VLPs (VP1+VP2). The CD spectra of VLPs (VP1+VP2) at pH 7 similar to that of VLPs (VP1) are not shown. At pH 8, the CD spectrum of VLPs (VP1+P2) underwent a minima shift from 205 nm to 202 nm, which differed from that of VLPs (VP1) with a shift from 205 nm to 200 nm.

centage of coil was increased from 32% to 36%. The CD spectrum at pH 8 shifted in minima from 205 nm to 202 nm, and this result differed from VLPs (VP1) at pH 8 with a shift in the minima from 205 nm to 200 nm.

The secondary structure stability of the two kinds of VLPs was similar in buffers at pH 2 to pH 7. At pH 8, VLPs (VP1+VP2) was more stable than VLPs (VP1) based on the CD analysis results of secondary structure percentages.

Discussion

Studies focusing on NoV have been hampered by the low amounts of this virus in stool samples obtained from infected individuals, along with the absence of a cell culture system and an animal model to propagate this virus (White *et al*., 1997). However, VLPs are spontaneously formed when NoV capsid protein VP1 is expressed in Sf9 cells infected with a recombinant baculovirus (Jiang *et al*., 1992). Although these VLPs are artificial products, they are morphologically and antigenically similar to the native virion (Jiang *et al*., 1992).

VP2 is characterized as a minor structural protein (Glass *et al*., 2000), and the expression of VP2 in insect cells yields two forms of protein: a 23 kDa unphosphorylated form and a 35 kDa phosphorylated form (Glass *et al*., 2000). VP2 is not essential for the formation of empty VLPs (Jiang *et al*., 1992; Green *et al*., 1997; White *et al*., 1997; Hale *et al*., 1999; Kobayashi *et al*., 2000). However, ORF3 is conserved in the genomes of caliciviruses, suggesting that this protein performs an important function in the life cycle of this virus (Glass *et al*., 2000). Furthermore, the absence of VP2 decreases the stability of VLPs when these particles are produced in insect cells (Bertolotti-Ciarlet *et al*., 2003). VP2 is possibly involved in viral assembly (Glass *et al*., 2000; Sosnovtsev *et al*., 2005). However, the mechanism by which protein VP2 increases the stability of VLPs remains unknown.

In this study, CD revealed the presence of VP2 that could partially stabilize the secondary structure of VLPs at pH 8. To determine the function of VP2 in the stability of VLPs,

we constructed and purified two kinds of VLPs from Sf9 cells infected with a recombinant baculovirus: one with VP2 and the other without VP2. We performed SDS-PAGE and western blot to determine the purity of VLPs and the presence of VP2 in VLPs. The result of SDS-PAGE of VLPs (VP1+VP2) only showed a 58 kDa protein band similar to VP1. The VP2 protein band was not observed. Western blot analysis results revealed the presence of VP2 in VLPs (VP1+VP2). These varied results may be due to the low copy number of VP2 approximately ranging from 1.5 to 8 per virion (Glass *et al*., 2000; Sosnovtsev *et al*., 2005; Luttermann and Meyers, 2007). The low concentration of VP2 in purified VLPs (VP1+VP2) may be insufficient and could not be detected by SDS-PAGE, even after the amount of sample was increased and Coomassie brilliant blue staining was replaced with silver staining (data not shown).

Both kinds of VLPs underwent structural changes at the secondary level induced by changes in pH. VLPs were incubated at pH 2 to pH 8 which fall within the pH range of the human gastrointestinal tract, where NoV should overcome drastic pH changes to reach and ultimately invade enteric cells. CD data revealed significant stability of the secondary structures of the two kinds of VLPs at neutral and acidic pH. By contrast, these secondary structures changed significantly at pH 8. These results are in agreement with those of Ausar *et al.* (2006) and White *et al.* (1997).

VLPs exhibited different behaviors at pH 2 to pH 7 and at pH 8, suggesting that pH-dependent characteristics are involved in the stability of virions *in vivo* (Ausar *et al*., 2006). As a gastrointestinal virus, NoV is spread via the fecal–oral route, indicating that the NoV particle should tolerate the highly acidic gastric juice of the host before this particle reaches its target organ (intestinal tract). Afterward, the virus migrates into the intestinal tract. Under alkaline pH conditions, virus particles become instable, and we presumed that this change possibly facilitated viral entry into intestinal epithelial cells and capsid disassembly to initiate virus replication. Such a stability-based switching mechanism that responds to subtle changes in the surrounding environment has been proposed for the tobacco mosaic virus (Culver 2002).

At pH 8, the secondary structure of VLPs (VP1) evidently changed. However, in VLPs (VP1+VP2), the change of the percentage of α-helix, β-sheet, β-turn, and coil was more moderate compared with VLPs (VP1). Considering the extremely low copy number of VP2 in VLPs (VP1+VP2) and the low protein concentration of VLPs (0.22 mg/ml) in CD analysis, we found that the lack of any detectable density could eliminate the possible effect of the secondary structure of VP2 on the percentage of the secondary structure elements of VLPs (VP1+VP2). This result was also confirmed by the same secondary structural data of VLPs (VP1+VP2) compared with those of VLPs (VP1) at pH 7. Therefore, VP2 could stabilize the secondary structure of VLPs (VP1+VP2) under alkaline pH conditions. This characteristic of VP2 indicates that this protein could enhance the stability of NoV in the intestinal tract of the host before the virus attaches to the intestinal epithelial cells and then starting its uncoading and replication process. Histo-blood group antigens (HBGAs) on cells of the human intestinal tract have been proposed to function as receptors of NoV (Marionneau *et al*., 2002; Lindesmith *et al*., 2003). Future research should be conducted to determine whether or not alkaline conditions in the intestinal tract can facilitate NoV recognition and attachment receptors and to clarify more mechanism of NoV entry.

Studies have suggested that VP2 is located in the interior of the capsid shell. The first isoleucine (Ile-52) in the IDPWI motif of the N-terminal arm of VP1, which is exceptionally conserved among NoV, is essential for VP1–VP2 interaction. The highly basic nature of VP2 and its location inside the viral particle are consistent with its potential function in assisting capsid assembly and genome encapsidation (Vongpunsawad *et al*., 2013). Our CD spectrum studies provided novel insights into the function of VP2 in the stability of VLPs. Future studies using structural techniques to determine three-dimensional structures will help elucidate the function of VP2. An improved understanding of the assembly/disassembly mechanisms possibly contribute to the development of strategies that aim to disrupt viral capsid formation.

Acknowledgements

This study was supported by the Promotive Research Fund for Excellent Young and Middle-Aged Scientists of Shandong Province (Grant No. BS2010SW041) and the National Natural Science Foundation of China (Grant No. 31101883).

References

Ando, T., Noel, J.S., and Fankhauser, R.L. 2000. Genetic classification of "Norwalk-like viruses". *J. Infect. Dis.* **181**, 336–348.

Atmar, R.L. and Estes, M.K. 2006. The epidemiologic and clinical importance of norovirus infection. *Gastroenterol. Clin. N. Am.* **35**, 275–290.

Ausar, S.F., Foubert, T.R., Hudson, M.H., Vedvick, T.S., and Middaugh, C.R. 2006. Conformational stability and disassembly of Norwalk virus-like particles: Effect of pH and temperature. *J. Biol. Chem.* **281**, 19478–19488.

Bertolotti-Ciarlet, A., Crawford, S.E., Hutson, A.M., and Estes, M.K. 2003. The 3′ end of Norwalk virus mRNA contains determinants that regulate the expression and stability of the viral capsid protein VP1: a novel function for the VP2 protein. *J. Virol.* **77**, 11603–11615.

Bertolotti-Ciarlet, A., White, L.J., Chen, R., Prasad, B.V., and Estes, M.K. 2002. Structural requirements for the assembly of Norwalk virus-like particles. *J. Virol.* **76**, 4044–4055.

Culver, J.N. 2002. Tobacco mosaic virus assembly and disassembly: determinants in pathogenicity and resistance. *Annu. Rev. Phytopathol.* **40**, 287–308.

Doultree, J.C., Druce, J.D., Birch, C.J., Bowden, D.S., and Marshall, J.A. 1999. Inactivation of feline calicivirus, a Norwalk virus surrogate . *J. Hosp. Infect.* **41**, 51–57.

Glass, P.J., White, L.J., Ball, J.M., Leparc-Goffart, I., Hardy, M.E., and Estes, M.K. 2000. Norwalk virus open reading frame 3 encodes a minor structural protein. *J. Virol.* **74**, 6581–6591.

Green, K.Y., Kapikian, A.Z., Valdesuso, J., Sosnovtsev, S., Treanor, J.J., and Lew, J.F. 1997. Expression and self-assembly of recombinant capsid protein from the antigenically distinct Hawaii human calicivirus. *J. Clin. Microbiol.* **35**, 1909–1914.

Hale, A.D., Crawford, S.E., Ciarlet, M., Green, J., Gallimore, C., Brown, D.W., Jiang, X., and Estes, M.K. 1999. Expression and self-assembly of Grimsby virus: antigenic distinction from Norwalk and Mexico viruses. *Clin. Diagn. Lab. Immunol.* **6**, 142–145.

Jiang, X., Matson, D.O., Ruiz-Palacios, G.M., Hu, J., Treanor, J., and Pickering, L.K. 1995. Expression, self-assembly, and antigenicity of a snow mountain agent-like calicivirus capsid protein. *J. Clin. Microbiol.* **33**, 1452–1455.

Jiang, X., Wang, M., Graham, D.Y., and Estes, M.K. 1992. Expression, self-assembly, and antigenicity of the Norwalk virus capsid protein. *J. Virol.* **66**, 6527–6532.

Jiang, X., Wang, M., Wang, K., and Estes, M.K. 1993. Sequence and genomic organization of Norwalk virus. *Virology* **195**, 51–61.

Karst, S.M., Wobus, C.E., Lay, M., Davidson, J., and Virgin, H.W.IV. 2003. STAT1-dependent innate immunity to a Norwalk-like virus. *Science* **299**, 1575–1578.

Kobayashi, S., Sakae, K., Suzuki, Y., Shinozaki, K., Okada, M., Ishiko, H., Kamata, K., Suzuki, K., Natori, K., Miyamura, T., and Takeda, N. 2000. Molecular cloning, expression, and antigenicity of Seto virus belonging to genogroup I Norwalk-like viruses. *J. Clin. Microbiol.* **38**, 3492–3494.

Kroneman, A., Harris, J.R., Vennema, H., Duizer, E., van Duynhoven, Y., Gray, J., Iturriza, M., Bottiger, B., Falkenhorst, G., Johnsen, C., and *et al.* 2008. Data quality of 5 years of central norovirus outbreak reporting in the European Network for food-borne viruses. *J. Public Health* **30**, 82–90.

Lindesmith, L., Moe, C., Marionneau, S., Ruvoen, N., Jiang, X., Lindblad, L., Stewart, P., LePendu, J., and Baric, R. 2003. Human susceptibility and resistance to Norwalk virus infection. *Nat. Med.* **9**, 548–553.

Luttermann, C. and Meyers, G. 2007. A bipartite sequence motif induces translation reinitiation in feline calicivirus RNA. *J. Biol. Chem.* **282**, 7056–7065.

Marionneau, S., Ruvoën, N., Le Moullac-Vaidye, B., Clement, M., Cailleau-Thomas, A., Ruiz-Palacois, G., Huang, P., Jiang, X., and Le Pendu, J. 2002. Norwalk virus binds to histo-blood group antigens present on gastroduodenal epithelial cells of secretor individuals. *Gastroenterology* **122**, 1967–1977.

Pirtle, E.C. and Beran, G.W. 1991. Virus survival in the environment. *Rev. Sci. Tech.* **10**, 733–748.

Prasad, B.V., Hardy, M.E., Dokland, T., Bella, J., Rossmann, M.G., and Estes, M.K. 1999. X-ray crystallographic structure of the Norwalk virus capsid. *Science* **286**, 287–290.

Sosnovtsev, S.V., Belliot, G., Chang, K.O., Onwudiwe, O., and Green, K.Y. 2005. Feline calicivirus VP2 is essential for the production of infectious virions. *J. Virol.* **79**, 4012–4024.

Svraka, S., Duizer, E., Vennema, H., de Bruin, E., van der Veer, B., Dorresteijn, B., and Koopmans, M. 2007. Etiological role of viruses in outbreaks of acute gastroenteritis in The Netherlands from 1994 through 2005. *J. Clin. Microbiol.* **45**, 1389–1394.

Vongpunsawad, S., Venkataram Prasad, B.V., and Estes, M.K. 2013. Norwalk virus minor capsid protein VP2 associates within the VP1 shell domain. *J. Virol.* **87**, 4818–4825.

Wang, D., Wu, Q., Kou, X., Yao, L., and Zhang, J. 2008. Distribution of norovirus in oyster tissues. *J. Appl. Microbiol.* **105**, 1966–1972.

White, L.J., Hardy, M.E., and Estes, M.K. 1997. Biochemical characterization of a smaller form of recombinant Norwalk virus capsids assembled in insect cells. *J. Virol.* **71**, 8066–8072.

Widdowson, M.A., Monroe, S.S., and Glass, R.I. 2005. Are noroviruses emerging? *Emerg. Infect. Dis.* **11**, 735–737.

Yang, J.T., Wu, C.S.C., and Martinez, H.M. 1986. Calculation of protein conformation from circular dichroism. *Methods Enzymol.* **130**, 208–269.

Zheng, D.P., Ando, T., Fankhauser, R.L., Beard, R.S., Glass, R.I., and Monroe, S.S. 2006. Norovirus classification and proposed strain nomenclature. *Virology* **346**, 312–323.